Modeling of Feedwater Heater in SMRs for Dynamic Simulation

Takhyun Chun [a], Gyudong Kim [a], Yong Jae Chae [a], Jeong Ik Lee [a*]
[a]*Department of Nuclear and Quantum Engineering, Korea Advanced Institute of Science and Technology (KAIST), 291 Daehak-ro, Yuseong-gu, Daejeon 34141, Republic of Korea*
[*]*Corresponding author: jeongiklee@kaist.ac.kr*

***Keywords :** FWH, MARS, Baffle flow, SMR

1. Introduction

According to the IEA's Electricity 2025 report [1], the power sector remains the largest contributor to global annual CO_2 emissions. In response, many countries are striving to increase the share of renewable energy in their power mix to mitigate this issue. However, electricity demand also exhibits significant variability throughout the day. Renewable sources such as solar PV and wind power are further constrained by their relatively low capacity factors, which undermines their ability to provide a stable supply. In this context, Small Modular Reactors (SMRs) have emerged as a compelling alternative for addressing demand fluctuations. Their compact, modular configuration offers several advantages, including improved safety, greater siting flexibility, and reduced construction risks. Moreover, SMRs typically achieve higher capacity factors than intermittent renewable sources, as shown in Table I, enabling them to deliver a more consistent and reliable supply of electricity. Therefore, load-following operation of SMRs is expected to play a critical role in ensuring the sustainability of renewable energy integration.

For load-following operation of SMRs, it is necessary to adopt operating strategies that account for the off-design characteristics of secondary system components such as turbines and feedwater heaters (FWHs). In addition, to ensure nuclear plant safety, the potential impacts of such strategies on the steam generator and the primary system must also be considered. To contribute to the realization of SMR load-following capability in response to the continuously increasing renewable energy capacity, this study develops a dynamic FWH model.

The key dynamic behaviors of the FWH that must be reflected in SMR simulations are as follows. First, during ramp-up and ramp-down, the timing of feedwater flow variation caused by the upstream pump differs from that of the turbine extraction steam flow entering the heater. Second, on the shell side, the high-temperature steam stream travels a longer effective path due to the presence of baffles. To capture these effects, an FWH model was constructed incorporating baffle flow. For this purpose, design parameters such as the number of tubes, number of baffles, pitch, and tube length were obtained.

Baffle flow consists of alternating cross-flow and window-flow regions, making it essential to account for the different contributions of these zones: heat transfer is dominated by cross-flow, while pressure drop is significantly influenced by window flow.

The FWH modeling was conducted using MARS-KS 2.0. The SMR layout used in this study is presented in Fig. 1, inspired by NuScale power cycle [2]. The steady-state parameters and performance of the SMR power cycle are summarized in Table II. The developed FWH model was calibrated to match the quasi-steady-state results of the SMR cycle, successfully reproducing cycle parameters such as Terminal Temperature Difference (TTD) and Drain Cooler Approach (DCA) [2]. These results are expected to support future transient analyses by enabling the dynamic response of FWHs to be reflected in SMR load-following operation.

Table I : Capacity factors of power sources [3]

Power source	Capacity factor	Installed capacity
Solar PV	0.13*	151.34 GW
Wind	0.20*	98.37 GW
SMR	0.86**	23.53 GW

* Average capacity factor from 2013 to 2022.
** Assume that the capacity factor of SMR is identical to that of commercial large-scale NPPs.

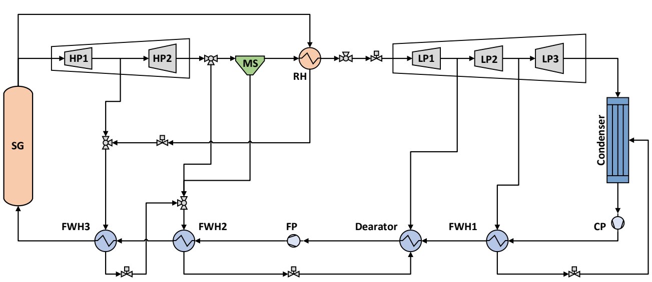

Fig. 1. Layout of SMR used in this study

Table II. Cycle parameters/conditions for on-design

Cycle Conditions	Value
SG thermal power	546 MWth
SG outlet pressure	5.25 MPa
SG outlet temperature	297.8 ℃
SG inlet temperature	230.0 ℃
Condenser outlet temperature	40 ℃
Hot side pressure drop	3% of inlet
Cold side pressure drop	2% of inlet
Cycle Parameters	Value
Turbine efficiency	92%
Pump efficiency	85%
Generator efficiency	96%
Turbine pressure ratio	2.41 for HPT
	287.98 for LPT
Reheater bypass ratio	0.0785
HPT work	38.9 MW
LPT work	150.3 MW
Feedwater pump work	2.3 MW
Feedwater mass flow rate	284.6 kg/s
Net efficiency	32.87 %

2. Geometry and Design Specifications

In this section, the closed FWH configuration employed in this study is described. Based on the EPRI guidelines [4], a representative FWH geometry commonly used in practice was selected. Feedwater flows on the tube side through U-shaped tubes, while the extraction steam flows on the shell side where baffles are installed.

2.1 FWH Type

A feedwater heater is typically divided into three functional zones—desuperheating, condensing, and drain cooling—each contributing to operational stability and heat transfer efficiency. The desuperheating zone reduces steam superheat to optimize utilization of the heat transfer surface, since the condensing zone exhibits superior heat transfer performance [4]. In this study, however, the desuperheating zone was omitted because the extraction steam entering the FWH was saturated, with no superheat present, as shown in Fig. 2.

In nuclear power plants, feedwater heaters are generally designed as horizontal, short-drain, and no-tube-in-window (NTIW) types. Horizontal heaters require more installation space but offer advantages in operation and maintenance, as accurate liquid level detection and control are critical for the drain cooler zone. Short-drain designs ensure that all tubes follow the same flow path, eliminating the need for flow distribution control required in partial-pass configurations [4]. Although the NTIW configuration increases cost due to its relatively low heat transfer coefficient and heat flux in the desuperheating zone, it effectively reduces the likelihood of failures caused by vibration and erosion in the window region, where flow reversal is significant [5].

2.2 Tube Diameter, Thickness, and Pitch

The tube outer diameter, thickness, and pitch were determined with reference to representative closed FWH design data [6-8]. Typical design values suitable for high-temperature and high-pressure conditions of approximately 300 °C and 55 bar were adopted, consistent with recommended standards. The tube outer diameter (OD) was set to 1 inch (25.4 mm), with a corresponding wall thickness of BWG 14 (2.11 mm). Stainless Steel 316 (SS316) was selected as the tube material. The tube pitch was specified as 1.5 times the OD, and the tubes were arranged in a triangular pitch with a 30° angle. The geometrical specifications of the FWH are summarized in Table III. The outer tube limit (D_{otl}) was determined based on clearance criteria relative to the inside shell diameter [9]. The tube-side velocity was also constrained to be below the maximum feedwater velocity criterion of 10 ft/s [6].

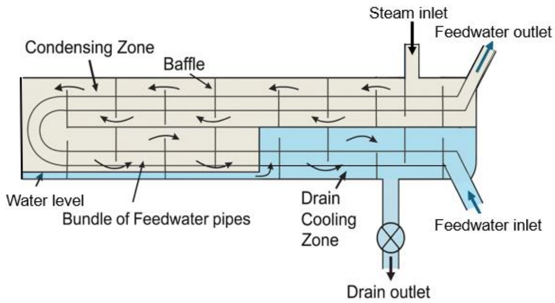

Fig. 2. Closed feedwater heater schematic

Table III. Geometrical parameters of FWH

Geometrical parameters	Value
Tube outer diameter (OD)	0.0254 m
Tube inner diameter	0.02118 m
Tube thickness	0.00211 m
Tube length	12.8 m
Pitch (P_T)	0.0381 m
Number of tubes	400
Inside shell diamter (D_s)	1.0 m
Outer tube limit (D_{otl})	0.982 m

3. Heat Transfer and Pressure Drop Analysis

The feedwater heater (FWH) analyzed in this study adopts a U-tube configuration, in which the feedwater flows inside the tubes and the turbine extraction steam flows on the shell side. On the shell side, baffles are installed to guide the steam flow, creating an alternating sequence of cross-flow and window-flow regions as shown in Fig. 3. This arrangement significantly influences both heat transfer and hydraulic performance. In the cross-flow regions, the steam is forced to move perpendicular to the tube bundle, which enhances heat transfer. In the window regions, however, the flow direction aligns more closely with the tubes, resulting in reduced heat transfer and a larger contribution to the overall pressure drop.

The FWH employed in this study is of the no-tube-in-window (NTIW) type, in which the feedwater tubes are not located in the window zones. Accordingly, effective heat transfer is assumed to occur only in the cross-flow regions, and thus only the cross-flow heat transfer characteristics were considered.

For the pressure drop, however, both the cross-flow and window zones must be taken into account. The total shell-side pressure drop can be expressed as the sum of the contributions from the central baffle spaces (cross-flow regions), the baffle window regions, and the entrance/exit regions.

$$\Delta P_w = \frac{\dot{m}_s^2}{S_m S_w \rho_s} \quad (1)$$

where,

ΔP_w = pressure drop in window zone

$\dot{m}_s$ = mass flow rate in shell side

S_m= cross-flow area

S_w= window flow area

ρ_s= density of the fluid in shell side

$$\Delta P_b = \frac{2 f_i \dot{m}_s^2 N_c}{S_m^2 \rho_s} \quad (2)$$

where,

ΔP_b = pressure drop in cross-flow zone

f_i= correction factor

For each zone, the pressure drop correlations were derived from the Modified Delaware Method [10] and applied to the alternating cross-flow and window-flow regions induced by the baffles. This approach ensures that both the heat transfer enhancement in the cross-flow region and the pressure loss in the window region are consistently represented.

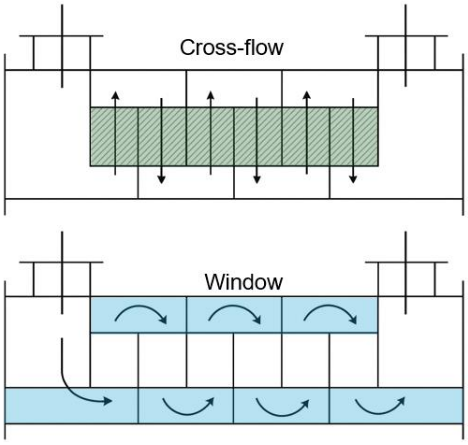

Fig. 3. Shell-Side Flow Regions of a Baffled FWH

4. Results and Discussions

Fig. 4 presents the axial temperature distribution of the feedwater and condensing steam within the third-stage feedwater heater (FWH). The horizontal axis indicates the axial position along the tube bundle, while the vertical axis shows the corresponding temperatures. Two distinct heat transfer regions can be identified: the drain cooling zone and the condensing zone. In the drain cooling zone, the feedwater temperature rises gradually due to heat exchange with the subcooled drain flow. In the condensing zone, the shell-side steam undergoes phase change at nearly constant temperature (approximately 235 °C).

The feedwater temperature profile shows that the temperature increase in the condensing zone is relatively steep. This indicates that the majority of heat transfer in the FWH occurs in the condensing zone, reflecting the higher heat transfer coefficient associated with condensation compared to single-phase heat transfer. These results highlight the importance of accurately modeling the condensation process in feedwater heaters. In the present modeling, the Terminal Temperature Difference (TTD) and Drain Cooler Approach (DCA) were calculated as 2.85 and 5.38, respectively, consistent with the design values, as depicted in Table IV.

The calculated pressure drop of the developed model was less than 0.1% of the shell-side pressure, which is consistent with the pressure drop ratios reported for the NuScale power cycle [2]. This negligible pressure drop indicates that the proposed geometry and baffle arrangement do not impose significant hydraulic penalties. Further, the results show that while cross-flow regions contribute primarily to heat transfer, window regions dominate the overall pressure loss, consistent with the Modified Delaware Method.

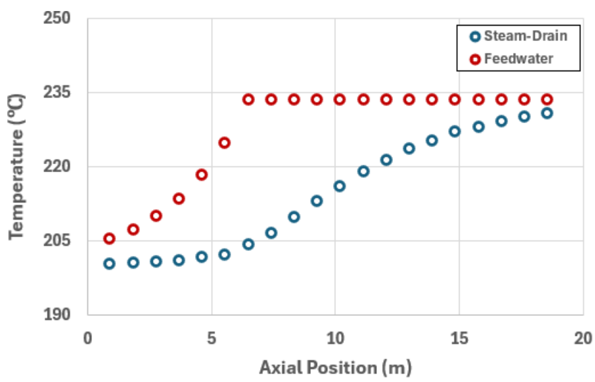

Fig. 4. Temperature profile in FWH 3rd stage

Table IV. Comparison of design values and MARS-KS values

Parameters	Design value (℃) [2]	MARS-KS value (℃)	Error (%)
TTD	5.7	5.38	5.61
DCA	2.9	2.85	1.72

5. Summary and Conclusions

In this study, the thermal-hydraulic characteristics of a closed feedwater heater (FWH) with a U-tube, horizontal, short-drain, and NTIW configuration were investigated. The geometry and design specifications were selected based on representative EPRI guidelines and typical high-pressure operating conditions. Heat transfer and pressure drop analyses were conducted by applying the Modified Delaware Method, with heat transfer considered only in the cross-flow regions in accordance with the NTIW assumption. The results demonstrate that the heat transfer process within the FWH is dominated by the condensing zone, where the shell-side steam undergoes phase change at nearly constant temperature. The steep increase in feedwater temperature in this region confirms the high effectiveness of condensation compared to single-phase convection. The drain cooling zone contributes to preheating of the feedwater, but its role is relatively limited compared to that of the condensing zone.

Furthermore, this study proposes a modeling approach that incorporates the extended shell-side flow path caused by baffle flow and relies on representative assumptions for the FWH geometry. Looking ahead, if the water level—an essential factor for FWH operational stability—is also integrated into the model, it would enable not only the representation of dynamic characteristics of FWHs during SMR load-following operation but also the evaluation of system stability.

The modeling framework in this study was established under thermohydraulic conditions representative of conventional PWR systems (e.g., SG outlet pressure of 5.25 MPa and outlet temperature of 297.8 °C). Accordingly, the proposed FWH model is most directly applicable to forced-circulation SMRs. Its extension to natural-circulation SMRs would require additional adjustments to account for their lower power ratings and different operating conditions.

Finally, variations in secondary-side power inevitably alter the outlet temperature of the FWH train, and hence the SG inlet temperature. This directly affects the thermal–hydraulic conditions of the primary system, implying that the FWH model cannot be considered fully independent of the reactor control logic. Therefore, while this study focuses on the secondary-side dynamics of the FWH, its practical application must account for the coupled interactions with the primary system during load-following operation.

ACKNOWLEDGEMENTS

This work was supported by the Small Modular Reactor Technology Development Program funded by the Korea government (MOTIE)(No. RS-2024-00400615).

REFERENCES

[1] IEA, *Electricity 2025*, International Energy Agency, Paris (2025).

[2] Chapter 10, *Steam and Power Conversion System*, in Nuclear Engineering Handbook, CRC Press, Boca Raton, 2016.

[3] Semin Joo, Seok Ho Song, Staffan Qvist, Jeong Ik Lee, "Evaluation of Coal Repowering Option with Small Modular Reactor in South Korea," *Energies*, 17, 6493 (2024).

[4] EPRI, *Feedwater Heater Maintenance Guide*, Electric Power Research Institute, Palo Alto, CA, Report No. 1003470, 2004.

[5] T. J. Muldoon, "Preventing Failures by Using No-Tube-in-the-Window (NTIW) Baffling in Feedwater Heater Design," *Proceedings of PWR2005, ASME Power*, Chicago, IL, USA, Apr. 5, 2005.

[6] HEI, *Standards for Closed Feedwater Heaters: 9th Edition*, Heat Exchange Institute, Cleveland, OH, 2015.

[7] TEMA, *Standards of the Tubular Exchanger Manufacturers Association: 9th Edition*, Tubular Exchanger Manufacturers Association, New York, 2007.

[8] T. Kuppan, *Heat Exchanger Design Handbook*, CRC Press, Boca Raton, FL, 2000.

[9] E. U. Schlunder (Ed.), *Heat Exchanger Design Handbook*, Hemisphere Publishing, Washington, DC, 1983.

[10] G. E. Weber and W. M. Worek, "Development of a Method to Evaluate the Design Performance of a Feedwater Heater With a Short Drain Cooler," ASME, Vol. 116, pp. 434–441, 1994.